Synthesis and Luminescent Properties of Eu^{3+} Doped Complex Borosilicate Glasses

Aneliya Yordanova , Margarita Milanova * , Lyubomir Aleksandrov , Reni Iordanova , Petia Petrova

Posted Date: 1 January 2026

doi: 10.20944/preprints202601.0022.v1

Keywords: glass; rare earths; photoluminescence; density

 doi:10.20944/preprints202601.0022.v1

Article

Synthesis and Luminescent Properties of Eu^{3+} Doped Complex Borosilicate Glasses

Aneliya Yordanova [1,2], Margarita Milanova [1,*], Lyubomir Aleksandrov [1,2], Reni Iordanova [1] and Petia Petrova [3]

[1] Institute of General and Inorganic Chemistry, Bulgarian Academy of Sciences, G. Bonchev Str., Bld. 11, 1113 Sofia, Bulgaria

[2] National Centre of Excellence Mechatronics and Clean Technologies, 8 bul., Kl. Ohridski, 1756 Sofia, Bulgaria

[3] Institute of Optical Materials and Technologies "Acad. Jordan Malinowski", Bulgarian Academy of Sciences, Blvd. Akad. G. Bonchev Str., Bld. 109, 1113 Sofia, Bulgaria

* Correspondence: margi@svr.igic.bas.bg

Abstract

Glasses with compositions $52.5B_2O_3$:$12.5SiO_2$:$25La_2O_3$:5CaO:5ZnO:$0.5Eu_2O_3$ and $50B_2O_3$:$10SiO_2$:$25La_2O_3$:5CaO:5ZnO:$5WO_3$:$0.5Eu_2O_3$ (mol%) were prepared by conventional melt-quenching method and investigated by X-ray diffraction analyses, DSC analysis, DR-UV-Vis spectroscopy and photoluminescence spectroscopy. Physical properties like density, molar volume, oxygen molar volume and oxygen packing density were also determined. Glasses are characterized with high glass transition temperature (over 650 °C). DR-UV-Vis spectroscopy results indicate that the tungstate ions incorporate into the base borosilicate glass as tetrahedral WO_4 groups. The lower band gap energy values show that the introduction of WO_3 into the base borosilicate glass increases the number of non-bridging oxygen species in the glass structure. The emission intensity of the Eu^{3+} ion increases with the introduction of WO_3 due to the occurrence of non-radiative energy transfer from the tungstate groups to the active ion. The most intense luminescence peak observed at 612 nm suggest that the glasses are potential materials for red emission.

Keywords: glass; rare earths; photoluminescence; density

1. Introduction

Over recent decades, the development and analysis of fluorescent materials doped with rare earth ions have garnered significant interest within the field of optoelectronics research. This growing attention stems from their wide array of applications in the creation and advancement of novel optical materials. Glasses, in particular, stand out as some of the most thoroughly studied engineering materials due to their versatility and adaptability achieved through composition modification. Additionally, they hold immense potential in innovations for optical communication and solid-state laser technologies [1]. Among the various types of glasses, borosilicate glasses have captured researchers' attention because of their remarkable properties. These include high chemical resistance, a high crystallization ability, lower thermal expansion, elevated softening temperature, and excellent mechanical strength. They are cost-effective and readily accessible. Such properties pave the way for extensive industrial applications in areas such as display technologies, solar energy systems, and MEMs technology.

In advanced technologies, trivalent rare earth ions play a pivotal role as active constituents in numerous optical materials. Their importance is owed to the presence of multiple absorption and emission bands that result from transitions between distinct energy levels. Notably, trivalent europium (Eu^{3+}) ions stand out as effective spectroscopic probes due to their simple energy-level structure, which features a non-degenerate $^7F_0$ ground state and $^5D_0$ excited state. This makes Eu^{3+}

 doi:10.20944/preprints202601.0022.v1

ions instrumental in studying the structure and chemical bonding nature within host matrices. Moreover, the strong $^5D_0$–$^7F_2$ electronic transition exhibited by these ions establishes them as efficient activators for generating intense red emission, particularly suited for display devices [1].

The study of borosilicate glasses doped with Eu_2O_3 oxide has been limited. Bi-containing borosilicate glasses doped with different amounts of Eu_3O_2 (1–5 mol%) were synthesized. The influence of the concentration of Eu_2O_3 on the physical, optical and luminescent properties of the glasses was studied. It was found that the glasses show the strongest emission at a wavelength of 613 nm and when excited by 465 nm. The color of the emission is reddish-orange. The optimal concentration of Eu_2O_3 in these glasses, at which the highest emission intensity is achieved, is 4.0 mol% [2]. Eu^{3+}-doped glasses with the composition $74.5B_2O_3$+$10SiO_2$+5MgO+R+$0.5Eu_2O_3$ [R=10 (Li_2O/Na_2O/K_2O)] are considered as potential candidates for red lasers, as well as for red color centers in displays [3]. Zinc-borosilicate glasses (with high ZnO content) doped with different amounts of Eu_2O_3 (0.2, 0.5, 1, 1.5, 2 mol %) were obtained. The glasses are characterized by intense red emission upon excitation with a wavelength of 395 nm. "Quenching" of the luminescence is observed at a concentration of Eu_2O_3 above 1 mol %. [4,5]. Thermally stable borosilicate glasses doped with Eu_2O_3 with the composition $35B_2O_3.20SiO_2.(15\text{-}x)Al_2O_3.15ZnO.15Na_2CO_3.xEu_2O_3$ (x = 0.5 ÷ 2.5 mol%) were synthesized.These glasses showed red emission, the intensity of which increased with increasing concentration of Eu^{3+} ions up to 2.5 mol% [6]. The effect of changing the concentration of B_2O_3 and Al_2O_3 in the composition of the glass Na_2O-Gd_2O_3-B_2O_3-SiO_2-Al_2O_3-Eu_2O_3 on the luminescent properties of the incorporated Eu^{3+} ions was studied. It was shown that with the addition of Al_2O_3, a $[BO_4] \rightarrow [BO_3]$ transformation occurs. The amorphous network becomes ''loose'', resulting in an increase in the space around the rare earth ions embedded in the glass matrix, an increase in their quenching concentration, and an improvement in the emission intensity of Eu^{3+} [7]. Physical, optical, and luminescent properties of Eu^{3+}-doped potassium borosilicate glasses (KBSi:Eu^{3+}) have been studied. The density and molar volume of the glasses increase with increasing Eu_2O_3 oxide content. After excitation with 394 nm, KBSi:Eu^{3+} glasses emit highly intense reddish-orange light and could find application in various photonic devices such as solid-state lasers and light-emitting diodes [8]. The optical and luminescent properties of Eu^{3+} doped $(55\text{-}x)B_2O_3$:$10SiO_2$:$25Y_2O_3$:10CaO:xEu_2O_3, x = 0 ÷ 2.5 mol% were studied [9]. The color coordinates of the glasses were found to be in the red region. The resulting glass is a potential candidate for red laser emission at 613 nm. Sm^{3+}/Eu^{3+} co-doped thermally stable zinc-alumino-borosilicate glasses and alkaline-earth-alumino-borosilicate glasses were investigated. They were shown to be suitable candidates for application as red components of white light emitting diodes [10,11]. Dy^{3+}/Eu^{3+} co-doped luminescent glasses SiO_2-B_2O_3-ZnO-La_2O_3-BaO (SBZLBA) were synthesized. When excited at 386 nm, the glasses exhibit three distinct emission regions: blue, yellow, and red, allowing for color-tunable luminescence ranging from cool white to neutral white and ultimately warm white by varying the excitation wavelength and Eu^{3+} doping concentration. Results indicate that Dy^{3+}/Eu^{3+} co-doped SBZLBa glasses are promising materials for white-light emitting devices [12]. Dy^{3+}/Eu^{3+} co-doped white-light emitting CaO-B_2O_3-SiO_2 glasses have been obtained. The glasses exhibit good thermal stability, and the luminescence color can be tuned by controlling the relative concentrations of Dy^{3+} and Eu^{3+} ions and the excitation wavelength. White light was achieved upon excitation at 387 nm when the concentrations of Dy^{3+} and Eu^{3+} were 4% and 2%, respectively [13].

It should be noted that in many cases the emission intensity of Eu^{3+} ions is higher when they are embedded in matrices containing tungsten oxide, compared to their intensity in other matrices. The significance of tungstates is determined by the occurrence of non-radiative charge transfer from WO_n groups to the active Re^{3+} (Nd, Sm, Eu, Tb, Dy) ion, which leads to an increase in the intensity and efficiency of the emission. There are very few studies in the literature on borosilicate glasses containing tungsten oxide, for example compositions: B_2O_3-SiO_2-ZnO-Na_2O-WO_3 [14] and $20B_2O_3$–$10SiO_2$–10CaO-$(60\text{-}x)Bi_2O_3$/xWO_3, x=0 to 20 wt% [15], which are mainly devoted to structural properties. There are no data on borosilicate glasses containing tungsten that are doped with Eu^{3+} ion.

 doi:10.20944/preprints202601.0022.v1

This work aims to investigate the influence of WO_3 on the physical parameters and luminescent characteristics of Eu^{3+} doped complex $(52.5-x/2)B_2O_3$:$(12.5-x/2)SiO_2$:$25La_2O_3$:$5ZnO$:$5CaO$:$0.5Eu_2O_3$:xWO_3, x= 0, 5 (mol%) glasses.

2. Results and Discussion

2.1. XRD Data and Thermal Analysis

The amorphous nature of the prepared materials was confirmed by X-ray diffraction analysis. Typical diffraction patterns of glasses obtained are shown in Figure 1. The photographic images (insets, Figure 1) show that transparent bulk glass specimens were obtained.

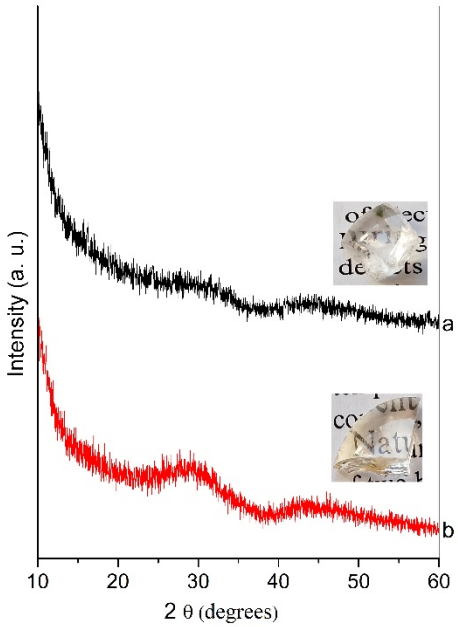

Figure 1. XRD patterns and photographs (insests) of investigated glasses: a) $52.5B_2O_3$:$12.5SiO_2$:$25La_2O_3$:$5ZnO$:$5CaO$:$0.5Eu_2O_3$;b)$50B_2O_3$:$10SiO_2$:$25La_2O_3$:$5ZnO$:$5CaO$:$0.5Eu_2O_3$:$5WO_3$.

$(52.5-x/2)B_2O_3$:$(12.5-x/2)SiO_2$:$25La_2O_3$:$5ZnO$:$5CaO$:$0.5Eu_2O_3$:xWO_3, x= 0, 5 (mol%) glasses have been also investigated by DSC analysis in order to obtain information for some thermal parameters and for structural changes that take place due to the compositional changes. The glass transition temperature, T_g, has been determined, since it is connected with both the strength of inter-atomic bonds and glass network connectivity. A higher T_g corresponds to a more rigid structure, whereas the glasses having a loose-packed structure have a lower T_g [16]. Figure 2 compares the DSC curves of the glasses investigated in this work.

 doi:10.20944/preprints202601.0022.v1

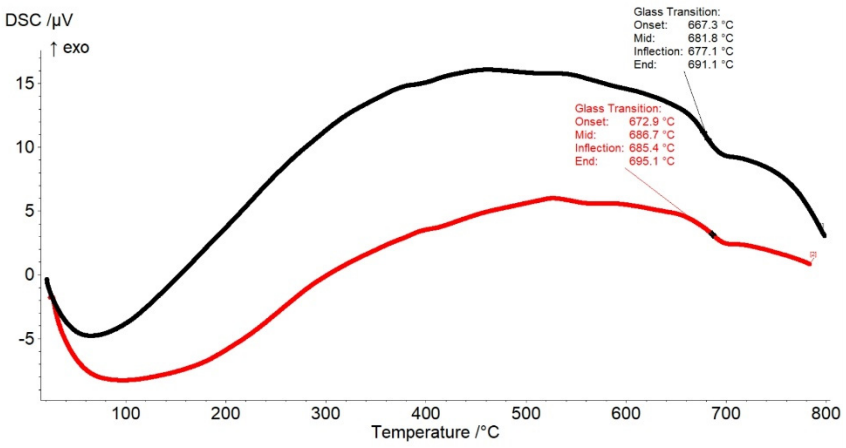

Figure 2. DSC curves of investigated glasses: $52.5B_2O_3$:$12.5SiO_2$:$25La_2O_3$:5ZnO:5CaO:$0.5Eu_2O_3$ (red line) $50B_2O_3$:$10SiO_2$:$25La_2O_3$:5ZnO:5CaO:$0.5Eu_2O_3$:$5WO_3$ (black line).

The endothermic dips corresponding to the glass transition temperature (T_g) are observed. As one can see, both glasses are characterized with high values of the glass transition temperature (T_g)—684.4 °C and 677.1 °C for WO_3-free and for WO_3-containing glass respectively, that is an indication of the formation of well packed glass structure. On the other hand, the addition of WO_3 into the base glass causes a slight decrease in the glass transition temperature values. We explain the observed reduction in T_g as a result of increasing non-bridging atoms with the addition of WO_3 [17].

2.2. DR-UV–vis spectra

UV–Vis spectroscopy was also applied for the characterization of the prepared material. Figure 3 shows the diffuse reflectance spectra of glasses obtained.

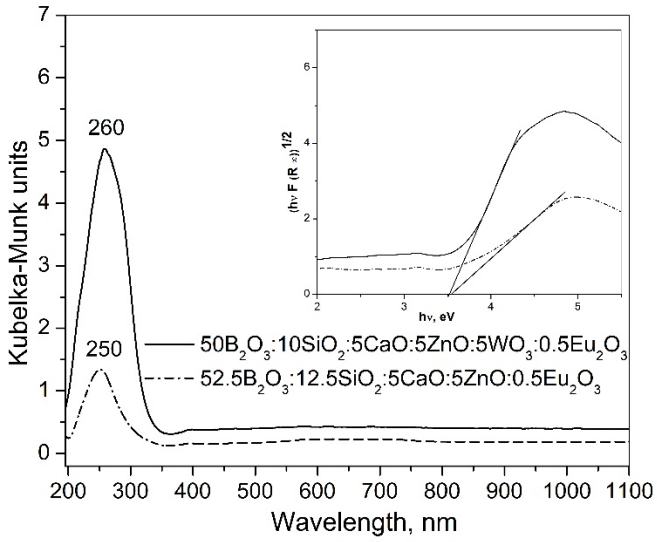

Figure 3. UV–vis optical spectra and Tauk plots (the insets) of investigated glasses.

In the spectrum of WO_3-free glass one symmetrical band at 250 nm is observed which is due to the presence of unavoidable trace iron impurities in the raw materials for glass preparation [18]. The optical absorption spectrum of the glass containing WO_3 displays one symmetrical high intensive band at 260 nm that can be assigned to the ligand–metal charge transfer (LMCT) from oxygen ligands to W^{6+} of distorted and isolated WO_4 tetrahedra. It is well known that UV-vis DRS for the isolated WO_4 reference compounds only possess a single ligand to-metal charge transfer (LMCT) band in the general region of 218-274 nm [19]. The exact location of this band maximum depends on the extent

 doi:10.20944/preprints202601.0022.v1

of distortion of the isolated WO_4 structure. For example, K_2WO_4 has a relatively undistorted isolated WO_4 unit and possesses a LMCT band at 223 nm, whereas $Zr(WO_4)_2$ consists of a distorted isolated WO_4 unit and exhibits a LMCT band at 274 nm. The absence of any absorption in the visible range indicates that W^{5+} species do not present in the investigated glasses [20]. Optical band gap values (E_g) evaluated from the UV–Vis spectra can give information about the structural arrangement of the glasses under investigation (inset of the Figure 3). The plot of transformed Kubelka–Munk function versus the energy of light (Tauc plot) provides band gap energies, E_g of 3.52 eV for WO_3-containing and 3.54 eV for WO_3-free glass samples respectively. According to the literature in glasses the variation of E_g may be attributed to the network structural changes. Generally, it is accepted that in metal oxides, creation of non-bonding orbitals with higher energy than bonding ones shifts valence band to higher energy which results to E_g decreasing [21]. Therefore, the increase in concentration of the NBOs (non-bridging oxygens) ions reduces the band gap energy. The lower band gap energy value for the WO_3 containing glass shows that introduction of WO_3 leads to the increase in number of non-bridging oxygen species in the glass structure.

2.3. Density, Molar Volume, Oxygen Packing Density and Oxygen Molar Volume

Higher number of non-bridging oxygen atoms in the network of WO_3-containing glass reveled by E_g values obtained are in line with the observed variation in density and various physical parameters established. The measured density of WO_3-free glass is 3.792 ± 0.002 g/cm^3, while the density of WO_3-containing glass increases to 3.973 ± 0.004 g/cm^3. This rise is attributed to substituting the lighter B_2O_3 (molecular weight 69.62 g/mol) and SiO_2 (molecular weight 60.08 g/mol) with the heavier WO_3 (molecular weight 231.84 g/mol) [22]. The molar volume also increases upon incorporating WO_3, changing from 35.38 cm^3/mol in WO_3—free glass to 35.87 cm^3/mol in WO_3—containing sample, which suggests that WO_3 expands the glass network. This expansion is linked to the difference in ionic radii between W^{6+} (0.6 Å) and B^{3+} (0.23 Å), and Si^{4+} (0.26 Å) creating additional free volume [23–25]. Oxygen molar volume (V_o) and OPD provide insight into how oxygen ions are packed within the glass structure [26]. Lower V_o and higher OPD values typically indicate a more tightly connected network. The WO_3 -containing glass shows a higher V_o (13.21 cm^3/mol) and lower OPD (75.69 g atom/l) compared to WO_3-free glass (13.15 cm^3/mol and 76.03 g atom/l, respectively), implying that WO_3 addition increases the concentration of non-bridging oxygens (NBOs) resulting in the formation of less packed and more disordered glass network.

2.4. Photoluminescent Properties

The excitation spectra of the prepared Eu^{3+} doped glasses are shown in Figure 4. All data were obtained at room temperature by monitoring the most intensive characteristic emission of Eu^{3+} ions at 612 nm wavelength, corresponding to $^5D_0 \rightarrow {}^7F_2$ transition. As can be seen from the figure, a broad, continuous band below 350 nm is observed, along with several narrow peaks distributed across the 350–600 nm wavelength range. Generally, the broadband is due to ligand to metal charge transfer transitions (LMCT) from oxygen 2p orbital to the empty 4f orbital of europium ($O^{2-} \rightarrow Eu^{3+}$) and from and $O^{2-} \rightarrow Zn^{2+}$ inside the ZnO_n (ZnO_n= ZnO_4) host absorbing groups [27–31]. Additionally, in the glass containing tungsten oxide ($50B_2O_3$:$25La_2O_3$:$10SiO_2$:$5CaO$:$5ZnO$:$5WO_3$:$0.5Eu_2O_3$) this band is also due to the transition from $O^{2-} \rightarrow W^{6+}$ inside the WO_n (WOn = WO_4 and WO_6) groups [32].

 doi:10.20944/preprints202601.0022.v1

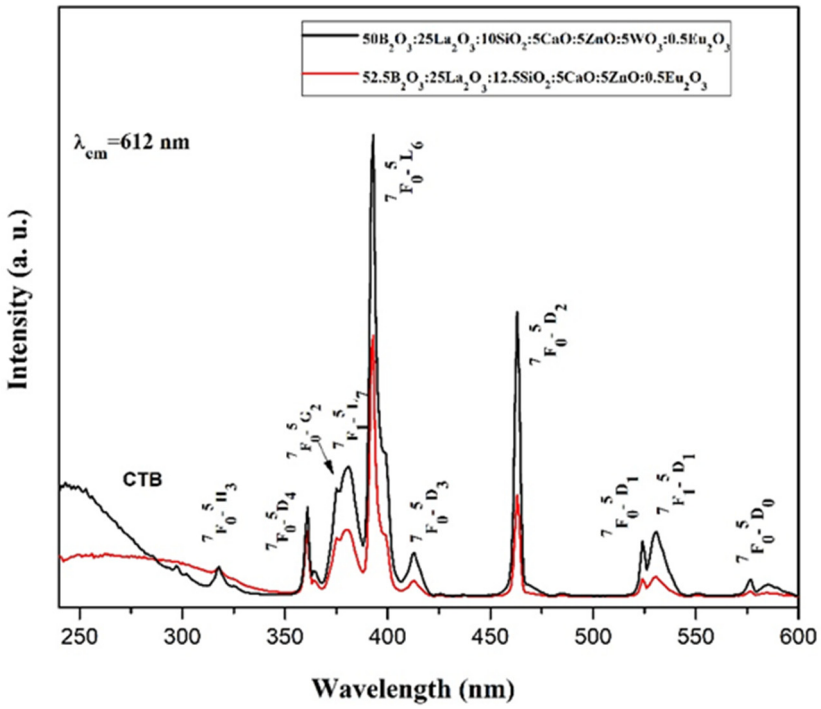

Figure 4. Excitation spectra of investigated glasses.

The presence of the excitation band of ZnO_n and WO_n, recorded at the emission wavelength of Eu^{3+} at 612 nm, suggests the existence of non-radiative energy transfer from the glass matrix to the luminescent rare-earth ion [32,33]. As can be observed from Figure 4, the glass containing WO_3 exhibits higher charge transfer absorption intensity. Consequently, WO_3 is expected to contribute significantly to the non-radiative energy transfer towards the luminescent Eu^{3+} ions, leading to stronger emission from the glass containing tungsten oxide. This mechanism is commonly referred to as host-sensitized luminescence. The distinct sharp peaks observed in the region above 350 nm are attributed to 4f–4f electron transitions from the ground state to excited energy levels, specifically $^7F_0 \rightarrow {}^5H_3$ (~318 nm), $^7F_0 \rightarrow {}^5D_4$ (~360 nm), $^7F_0 \rightarrow {}^5G_2$ (~376 nm), $^7F_1 \rightarrow {}^5L_7$ (~381 nm), $^7F_0 \rightarrow {}^5L_6$ (~393 nm), $^7F_0 \rightarrow {}^5D_3$ (~413 nm), $^7F_0 \rightarrow {}^5D_2$ (~463 nm), $^7F_0 \rightarrow {}^5D_1$ (~523 nm) and $^7F_1 \rightarrow {}^5D_1$ (~531 nm), $^7F_0 \rightarrow {}^5D_0$ (~576 nm). The highest excitation was observed at $^7F_0 \rightarrow {}^5L_6$ (393 nm). Therefore, the emission spectra measurements were conducted under excitation at 393 nm. The comparison between the LMCT band and the 4f–4f transitions reveals that the narrow Eu^{3+} peaks exhibit higher intensity. This means that the efficient excitation by near-UV and blue LED chips can be obtained, since Eu^{3+} 4f–4f transitions are typically weak because they are partially forbidden by Laporte's selection rule [34].

The emission spectra of Eu^{3+} doped borosilicate glasses (Figure 5) were recorded at room temperature using 393 nm excitation wavelength. The five narrow characteristic emission peaks, originating from the radiative transitions of Eu^{3+} ions from the $^5D_0$ excited state to the lower-lying $^7F_0$, $^7F_1$, $^7F_2$, $^7F_3$, $^7F_4$ ground states are observed at 578 nm, 591 nm, 612 nm, 652 nm and 701 nm [35]. As shown in Figure 5 the emission intensity exhibits a strong dependence on the composition and increases with the incorporation of tungsten in glass matrix. This behaviour can be related to non-radiative charge-transfer processes between the glass host and the luminescent Eu^{3+} ions.

Additional evidence for this energy-transfer mechanism is provided by the absence of the typical broad WO_3 band in the 400-600 nm [36] spectral region, indicating that the excitation energy absorbed by tungstate groups is efficiently transferred non-radiatively to the Eu^{3+} ions. The absence of ZnO emission bands [37] in the same region is also suggesting energy transfer, but to a lesser extent. Among all the observed emission bands, the most intense one, centered at 612 nm, originates from the forced electric-dipole (ED) $^5D_0 \rightarrow {}^7F_2$ transition, which is highly sensitive of the local crystal-field environment surrounding the Eu^{3+} ions, followed by the magnetic-dipole (MD) $^5D_0 \rightarrow {}^7F_1$ at 591 nm

 doi:10.20944/preprints202601.0022.v1

transition, which is insensitive to the surrounding ligands [27,35]. The dominance of the ED transition over the MD transition indicates that Eu^{3+} ions occupy non-centrosymmetric sites within the glass host. Moreover, the ratio of these emission intensities, commonly referred to the asymmetry ratio R=($^5D_0 \rightarrow {}^7F_2$)/($^5D_0 \rightarrow {}^7F_1$), provides insight into the degree of local asymmetry surrounding around the Eu^{3+} ions as well as the strength of Eu–O covalence in various Eu^{3+}-doped materials [38,39]. Lower values of the asymmetry parameter correspond to higher local site symmetry around the active ion, lower Eu–O covalency and emission intensity. The increase in R value is due to the increase in asymmetry and covalency between the Eu^{3+} ion and the ligands and leads to a higher emission intensity [40]. The R values of the synthesized glasses are listed in Table 1 along with other data reported in the literature for Eu^{3+}-doped glasses and the commercial used phosphor material.

Table 1. Comparison of Intensity Ratio R of Eu^{3+} doped borosilicate glasses with different host matrices.

Glass Composition	Relative Intensity Ratio, R	Reference
$52.5B_2O_3$:$25La_2O_3$:$12.5SiO_2$:5CaO:5ZnO:$0.5Eu_2O_3$	4.12	Current work
$50B_2O_3$:$25La_2O_3$:$10SiO_2$:5CaO:5ZnO:$5WO_3$:$0.5Eu_2O_3$	4.42	Current work
50ZnO:(49–x)B_2O_3:1Bi_2O_3:xWO_3: $0.5Eu_2O_3$ x = 1, 5, 10,	4.61-5.73	41
50ZnO:40B_2O_3:10WO_3:xEu_2O_3 (0≤x≤10)	4.54÷5.77	42
50ZnO:(50–x)B_2O_3:xNb_2O_5:$0.5Eu_2O_3$:, x= 0, 1, 3 and 5 mol%	4.31-5.16	43
50ZnO:(50−x)B_2O_3:$0.5Eu_2O_3$:xWO_3, x = 0, 1, 3, 5.	4.34-5.57	17
$89.5B_2O_3$–$10Li_2O$–$0.5Eu_2O_3$	2.41	44
$64SiO_2$-16K_2O-16BaO-$4Eu_2O_3$	3.42	
$0.5GeO_2$-$63.5SiO_2$-16K_2O-16BaO-$4Eu_2O_3$	3.46	
4ZnO:$3B_2O_3$ 0.5–2.5 mol % Eu_2O_3	2.74-3.94	45
60ZnO:$20B_2O_3$:(20 − x)SiO_2–xEu_2O_3 (x = 0 and 1)	3.166	46
74.5 B_2O_3+$10SiO_2$+5 MgO+5x+$0.5 Eu_2O_3$, x= Li_2O+Na_2O; Li_2O+K_2O and K_2O+Na_2O	2.102-2.266	47
20 MF_2·69 B_2O_3·10 Al_2O_3·$1Eu_2O_3$, *M* = Ca, Pb and Zn	3.77-5.89	48
$35B_2O_3$–$20SiO_2$-(15-x) Al_2O_3–15ZnO-$15Na_2CO_3$-xEu_2O_3 (x = 0.0, 0.5, 1.0, 1.5, 2.0, 2.5 mol%)	3.62–3.92	49
$50B_2O_3$-$19SiO_2$-$20Na_2O$-10CaO-$1Eu_2O_3$	3.151	50
$50B_2O_3$-$14SiO_2$-$20Na_2O$-10CaO-5ZnO-$1Eu_2O_3$	3.352	
$50B_2O_3$-$14SiO_2$-$20Na_2O$-10CaO-$5TeO_2$-$1Eu_2O_3$	4.269	
Eu^{3+}:Y_2O_3	3.8-5.2	51, 52

Compared to our previous synthesized glasses containing boron and tungsten oxides, the values of the asymmetric ratio R are similar [17,41–43], but compared to other borate or silicate oxide glass compositions [44–50] the values are higher. The relatively higher R values observed in the present glasses indicate that Eu^{3+} ions occupy low-symmetry crystallographic sites and provide evidence of the high Eu^{3+}-O^{2-} covalency. The higher asymmetry ratio, 4.42, obtained for the tungsten containing glass composition $50B_2O_3$:$25La_2O_3$:$10SiO_2$:5CaO:5ZnO:$5WO_3$:$0.5Eu_2O_3$, suggests stronger emission intensity compared to the WO_3 free glass. In addition, the $^5D_0 \rightarrow {}^7F_1$ transition of Eu^{3+} exhibits splitting into three emission peaks. This behaviour is attributed to crystal-field-induced splitting, where a single electronic transition gives rise to multiple emission components [53]. Moreover, the presence of the $^5D_0 \rightarrow {}^7F_0$ transition, which is highly sensitive to the local crystal field and normally forbidden under standard Judd–Ofelt theory, further confirms that Eu^{3+} ions reside at non-centrosymmetric sites with C_{2v}, C_n, or C_s symmetry within the glass matrix [54]. Further to evaluate the luminescent properties and the perceived emission color, the Commission Internationale de l'Éclairage (CIE) 1931 chromaticity diagram was used [55]. The chromaticity coordinates of the synthesized borosilicate glasses were calculated from the photoluminescence spectra (Figure 5) using SpectraChroma software (Version 1.0.1, CIE coordinate calculator) [56]. The obtained values are almost identical and

 doi:10.20944/preprints202601.0022.v1

are located within the red region of the CIE diagram (Figure 6) and are summarized in Table 2. The calculated coordinates are very close to the NTSC standard for red light (0.670, 0.330) as well as to the chromaticity coordinates of the commercial red phosphor $Y_2O_2S:Eu^{3+}$ (0.658, 0.340) [57].

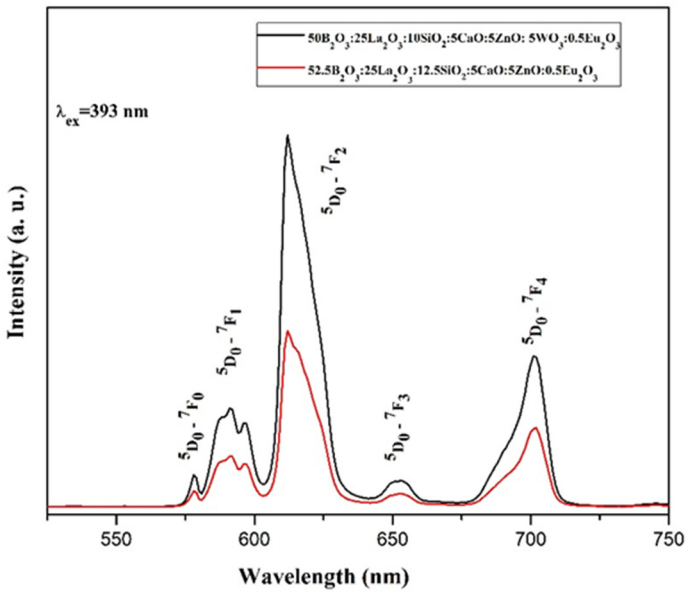

Figure 5. Emission spectra of investigated glasses.

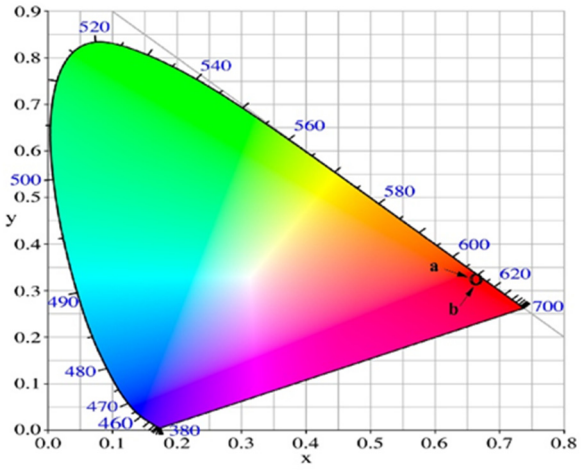

Figure 6. CIE chromaticity diagram of investigated glasses: (a) 52.5 B_2O_3:25La_2O_3:12.5SiO_2:5CaO:5ZnO:0.5Eu_2O_3; (b) 50B_2O_3:25La_2O_3:10SiO_2:5CaO:5ZnO:5WO_3:0.5Eu_2O_3.

Table 2. CIE chromaticity coordinates of the borosilicate glasses.

Glass Composition	Chromaticity Coordinates (x, y)
52.5 B_2O_3:25La_2O_3:12.5SiO_2:5CaO:5ZnO:0.5Eu_2O_3	0.649, 0.348
50B_2O_3:25La_2O_3:10SiO_2:5CaO:5ZnO:5WO_3:0.5Eu_2O_3	0.652, 0.348
NTSC standard for red light	0.670, 0.330
$Y_2O_2S:Eu^{3+}$	0.658, 0.340

3. Materials and Methods

Two glass samples of 52.5B_2O_3:12.5SiO_2:25La_2O_3:5CaO:5ZnO:0.5Eu_2O_3 and 50B_2O_3:10SiO_2:25La_2O_3:5CaO:5ZnO:5WO_3:0.5Eu_2O_3 compositions (in mol%) were obtained by applying of the melt quenching method, using reagent grade La_2O_3, H_3BO_3, SiO_2, CaO, ZnO and WO_3

 doi:10.20944/preprints202601.0022.v1

as raw materials. The homogenized batches were melted at 1400 °C for 2 hours in a curundum crucible in air. The melts were cast into preheated graphite mold to get bulk glass samples. Then the glasses were transferred in a laboratory electric furnace annealed at 500 °C for 1hour and then were cooldown to room temperature at a very slow cooling rate of about 0.5 °C/min. The phase formation of the samples was established by x-ray phase analysis with a Bruker D8 Advance diffractometer, using Cu Kα radiation in the $10 < 2\theta < 60$ range. The glass transition (T_g) temperatures of the glasses were determined by differential scanning calorimetry (DSC) using a Netzsch 404 Pegasus instrument, 2021 Selb, Germany, at a heating rate of 10 K/min in an Ar flow of 10 mL/s, using corundum crucibles with lids. The density of the obtained glasses at room temperature was measured by the Archimedes principle using toluene ($\varrho = 0.867$ g/cm^3) as an immersion liquid on a Mettler Toledo electronic balance of sensitivity 10^{-4} g. From the experimentally evaluated density values the molar volume (V_m), the molar volume of oxygen (V_o) (volume of glass in which 1 mol of oxygen is contained) and the oxygen packing density (OPD) of glasses obtained were estimated, using the following relations respectively:

$$\mathbf{V_m} = \frac{\Sigma \mathbf{x_i M_i}}{\boldsymbol{\rho_g}} \quad (1)$$

$$\mathbf{V_o} = \mathbf{V_m} \times \left(\frac{\mathbf{1}}{\Sigma \mathbf{x_i n_i}}\right) \quad (2)$$

$$\mathbf{OPD} = \mathbf{1000} \times \mathbf{C} \times \left(\frac{\rho_g}{\mathbf{M}}\right) \quad (3)$$

where x_i is the molar fraction of each component i, M_i the molecular weight, ϱ_g the glass density and n_i is the number of oxygen atoms in each oxide, C is the number of oxygen per formula units, and M is the total molecular weight of the glass compositions. The optical spectra of the powder samples at room temperature were recorded with a spectrometer (Evolution 300 UV–vis Spectrophotometer) employing the integration sphere diffuse reflectance attachment. The samples were measured in the wavelength (λ) range of 200–1100 nm with a magnesium oxide reflectance standard used as the baseline. The uncertainty in the observed wavelength is about ±1 nm. The Kubelka–Munk function ($F(R\infty)$) was calculated from the UV–Vis diffuse reflectance spectra. The band gap energy (E_g) was determined by plot $(F(R\infty)\ h\nu)^{1/n}$, n = 2 versus hν (incident photon energy). Photoluminescence(PL) excitation and emission spectra at room temperature for all glasses were measured with a Spectrofluorometer FluoroLog3-22, 2014 (Horiba JobinYvon,).

4. Conclusions

In this study the influence of WO_3 on the physical parameters and luminescent characteristics of Eu^{3+} doped complex borosilicate glasses $(52.5\text{-}x/2)B_2O_3$:$(12.5\text{-}x/2)SiO_2$:$25La_2O_3$:$5ZnO$:$5CaO$:$0.5Eu_2O_3$:xWO_3, x = 0, 5 (mol%) was established. The XRD results confirmed the amorphous nature of the glasses. The optical absorption spectra contained a major band corresponding to W^{6+} ions in tetrahedral positions. The decrease in both the optical band gap and the glass transition temperature, and variation in the physical parameters indicated the decrease in the degree of polymerization (increasing number of non-bridging oxygen atoms) with the addition of 5 mol% WO_3 into the base complex borosilicate glass. The positive effect of WO_3 on the luminescence intensity of the Eu^{3+} doped complex borosilicate glass was established. The high luminesce intensity ratio (R) = $(^5D_0\text{-}^7F_2)/(^5D_0\text{-}^7F_1)$ and color chromaticity coordinate (0.652, 0.348) support that, Eu^{3+} doped borosilicate glass, having 5 mol. % WO_3 is a suitable candidate for visible red emission applications.

Author Contributions: Conceptualization, M.M. and A.Y.; methodology, M.M., A.Y., L.A. and R.I.; investigation, M.M., A.Y., L.A. and P.P.; writing—original draft preparation, M.M. and A.Y.; writing—review and editing, R.I. All authors have read and agreed to the published version of the manuscript.

Funding: This research received no external funding.

 doi:10.20944/preprints202601.0022.v1

Institutional Review Board Statement: Not applicable.

Data Availability Statement: Data are contained within the article. Further inquiries can be directed to the corresponding author.

Acknowledgments: This work is supported by the European Regional Development Fund under the "Research Innovation and Digitization for Smart Transformation" program 2021–2027 under the Project BG16RFPR002-1.014-0006 at the National Centre of Excellence for Mechatronics and Clean Technologies.

Conflicts of Interest: The authors declare no conflicts of interest.

References

1. Reddy, B. N. K.; Raju, B. D.; Thyagarajan, K.; Ramanaiah, R.; Jho, Y. D. B. Reddy, S. Optical characterization of Eu3+ ion doped alkali oxide modified borosilicate glasses for red laser and display device applications. *Ceram. Int.* **2017**, *43* (12), 8886-8892.
2. Rakpanicha, S.; Wantana, N.; Kaewkhao, J. Development of bismuth borosilicate glass doped with Eu^{3+} for reddish orange emission materials application. *Mater. Today: Proc.* **2017**, *4*, 6389–6396.
3. Reddy, B. N. K.; Raju, B. D.; Thyagarajan, K.; Ramanaiah, R.; Jhod, Y. D.; Reddy, B. S. Optical characterization of Eu^{3+} ion doped alkali oxide modified borosilicate glasses for red laser and display device applications. *Ceram. Int.* **2017**, *43*, 8886–8892.
4. Hussain, N. S.; Reddy, Y. P.; Buddhudu, S. Luminescence properties of Eu^{3+} doped $ZnO–B_2O_3–SiO_2$ glasses. *Spectrosc. Lett.* **2002**, *35*, 275–283.
5. Cheong, W. M.; Zaid, M. H. M.; Matori, K. A.; Fen, Y. W.; Tee, T. S.; Loh, Z. W.; Mayzan, M. Z. H. Promising reddish-orange light as Eu^{3+} incorporated in zinc-borosilicate glass derived from the waste glass bottle. *J. Taibah Univ. Sci.* **2023**, *17*, 2260080.
6. Bajaj, R.; Rao, A. S.; Prakash, G. V. Photoluminescence down-shifting studies of thermally stable Eu^{3+} ions doped borosilicate glasses for visible red photonic device applications. *J. Non-Cryst. Solids* **2022**, *575*, 121184.
7. Hu, G.; Zhou, Y.; Liu, R.; Li, C.; Liu, L.; Lin, H.; Zeng, F.; Su, Z. Regulation of luminescence properties of SBGNA:Eu^{3+} glass by the content of B_2O_3 and Al_2O_3. *Opt. Mater.* **2020**, *106*, 110025.
8. Rakpanich, S.; Wantana, N.; Ruangtaweep,Y.; Kaewkhao, J. Eu^{3+} doped borosilicate glass for solid-state luminescence material. *J. Met. Mater. Miner.***2017**, *27*, 35–38.
9. Aryal, P.; Kesavulu, C. R.; Kim, H. J.; Lee, S. W.; Kang, S. J.; Kaewkhao, J.; Chanthima, N.; Damdee, B. Optical and luminescence characteristics of Eu^{3+}-doped B_2O_3:SiO_2:Y_2O_3:CaO glasses for visible red laser and scintillation material applications. *J. Rare Earths* **2018**, *36*, 482–491.
10. Ravita, A.; Rao, S. Effective sensitization of Eu^{3+} visible red emission by Sm^{3+} in thermally stable potassium zinc alumino borosilicate glasses for photonic device applications. *J. Lumin.* **2022**, *244*, 118689.
11. Sharma, S.; Rao, A. S.; Kishore, K. Energy transfer dynamics in thermally stable Sm^{3+}/Eu^{3+} co-doped AEAlBS glasses for near UV triggered photonic device applications. *J. Non-Cryst. Solids* **2022**, *580*, 121392.
12. Jin, Z.; Zhu, Z. Luminescence and spectroscopic studies on Dy^{3+}–Eu^{3+} doped $SiO_2–B_2O_3–ZnO–La_2O_3–BaO$ glass for WLED. *J. Non-Cryst. Solids* **2024**, *641*, 123153.
13. Zhou, W.; Wang, G.; Zheng, X.; Yu, L.; Zhang, J.; Qiu, Z.; Lian, S. Tunable colors and applications of Dy^{3+}/Eu^{3+} co-doped $CaO–B_2O_3–SiO_2$ glasses. *J. Am. Ceram. Soc.* **2019**, *102(10)*, 5890-5898.
14. Alsafi, K.; Ismail, Y. A.; Aloraini, D. A.; Almutairi, H. M.; Al-Saleh, W. M.; Shaaban, K. S. Exploring the radiation shielding properties of $B_2O_3–SiO_2–ZnO–Na_2O–WO_3$ glasses: a comprehensive study on mechanical, gamma, and neutron attenuation characteristics. *Prog. Nucl. Energy* **2024**, *170*, 105151.
15. Ali, A. S.; Alrowaily, A. W.; Issa, S. A.; Rashad, M.; Elsaman, R.; Zakaly, H. M. Unveiling the structural, optical, and electromagnetic attenuation characteristics of $B_2O_3–SiO_2–CaO–Bi_2O_3$ glasses with varied WO_3 content. *Radiat. Phys. Chem.* **2023**, *212*, 111089.
16. Ray, N.H. Composition-properties relationship in Inorganic Oxide Glasses. *J. Non-Cryst. Solids* **1974**, *15*, 423–434.
17. Yordanova, A.; Aleksandrov L.; Milanova M.; Iordanova R.; Petrova P.; Nedyalkov N. Effect of the Addition of WO_3 on the Structure and Luminescent Properties of ZnO-B_2O_3:Eu^{3+} Glass. *Molecules* **2024**, *29(11)*, 2470.

 doi:10.20944/preprints202601.0022.v1

18. ElBatal, F. H.; Selim, M., S.; Marzouk, S. Y.; Azooz, M. A. UV-vis absorption of the transition metal-doped SiO_2-B_2O_3-Na_2O_3 glasses. *Phys. B* **2007**, *398*, 126-134.
19. Ross-Medgaarden, E. I.; Wachs, I. E. Structural Determination of Bulk and Surface Tungsten Oxides with UV-vis Diffuse Reflectance Spectroscopy and Raman Spectroscopy. *J. Phys. Chem. C* **2007**, *111*, 15089-15099.
20. Ouis, M.; El-Batal, H. A.; Azoz, M.; Abdelghany, A. *Indian J. Pure Appl. Phys.* **2013**, *51*, 11–17.
21. Rani, S.; Sanghi, S.; Ahlawat, N.; Agarwal, A. Influence of Bi_2O_3 on thermal, structural and dielectric properties of lithium zinc bismuth borate glasses. *J. Alloys Comp.* **2014**, *597*, 110–118.
22. Bajaj, A.; Khanna, A.; Kulkarni, N.K.; Aggarwal, S.K. Effects of Doping Trivalent Ions in Bismuth Borate Glasses. *J. Am. Ceram. Soc.* **2009**, *92*, 1036–1041.
23. Saranya, S.; Balakrishnan, L.; Sangeetha, D.; Lakshmi Priya, S. Investigating the effects of Hg doping on WO3 nanoflakes: a hydrothermal route to tailored properties. *Dig. J. Nanomater. Biostruct.* **2025**, *20(2)*, 669–679.
24. Zhao D.; Yu, Y.; Cao, C.; Wang, J.; Wang, E.; Cao; Y. The existing states of doped B^{3+}ions on the B doped TiO_2. *Appl. Surf. Sci.* **2015**, *345*, 67-71.
25. Stevenson, A. J.; Li, X.; Martinez, M. A.; Anderson, J. M.; Suchy, D.L.; Kupp, E. R.; Dickey, E. C.; Mueller, K. T.; Messing, G. L. Effect of SiO_2 on Densification and Microstructure Development in Nd:YAG Transparent Ceramics. *J. Am. Ceram. Soc.* **2011**, *94 (5)*, 1380–1387.
26. Villegas, M.A.; Navarro, J.M.F. Physical and structural properties of glasses in the TeO_2–TiO_2–Nb_2O_5 system. *J. Eur. Ceram. Soc.* **2007**, *27 (7)*, 2715–2723.
27. Blasse, G.; Grabmaier, B.C. Luminescent Materials, 1st ed.; Springer: Berlin/Heidelber, Germany, **1994**; p. 18.
28. Hoefdraad, H.E. The charge-transfer absorption band of Eu^{3+} in oxides. *J. Solid State Chem.* **1975**, *15*, 175–177.
29. Parchur, A.K.; Ningthoujam, R.S. Behaviour of electric and magnetic dipole transitions of Eu^{3+}, $^5D_0$-$^7F_0$ and Eu-O charge transfer band in Li^+ co-doped YPO_4:Eu^{3+}. *RSC Adv.* **2012**, *2*, 10859–10868.
30. Mariselvam, K.; Liu, J. Synthesis and luminescence properties of Eu^{3+} doped potassium titano telluroborate (KTTB) glasses for red laser applications. *J. Lumin.* **2021**, *230*, 117735.
31. Nimpoeno, W.A.; Lintang, H.O.; Yuliati, L. Zinc oxide with visible light photocatalytic activity originated from oxygen vacancy defects. *IOP Conf. Ser. Mater. Sci. Eng.* **2020**, *833*, 012080.
32. Dutta, P.S.; Khanna, A. Eu^{3+} activated molybdate and tungstate based red phosphors with charge transfer band in blue region. *ECS J. Solid State Sci. Technol.* **2013**, *2*, R3153–R3167.
33. Thieme, C.; Herrmann, A.; Kracker, M.; Patzig, C.; Hoche, T.; Russel, C. Microstructure investigation and fluorescence properties of Europium-doped scheelite crystals in glass-ceramics made under different synthesis conditions. *J. Lumin.* **2021**, *238*, 118244.
34. Bunzli, J.C.G. Lanthanide luminescence: From a mystery to rationalization, understanding, and applications. In Handbook on the Physics and Chemistry of Rare Earths; Elsevier: Amsterdam, The Netherlands, **2016**; Volume *50*, pp. 141–176.
35. Binnemans, K. Interpretation of europium (III) spectra. *Coord. Chem. Rev.* **2015**, *295*, 1–45.
36. Sungpanich, J.; Thongtem, T.; Thongtem, S. Large-scale synthesis of WO_3 nanoplates by a microwave-hydrothermal method. *Ceram. Int.* **2012**, *38*, 1051–1055.
37. Nimpoeno,W.A.; Lintang, H.O.; Yuliati, L. Zinc oxide with visible light photocatalytic activity originated from oxygen vacancy defects. *IOP Conf. Ser. Mater. Sci. Eng*. **2020**, *833*, 012080.
38. Devi, C.H.B.; Mahamuda, S.; Swapna, K.; Venkateswarlu, M.; Rao, A.S.; Prakash, G.V. Compositional dependence of red luminescence from Eu^{3+} ions doped single and mixed alkali fluoro tungsten tellurite glasses. *Opt. Mater.* **2017**, *73*, 260–267.
39. Nogami, M.; Umehara, N.; Hayakawa, T. Effect of hydroxyl bonds on persistent spectral hole burning in Eu^{3+} doped BaO-P_2O_5 glasses. *Phys. Rev. B* **1998**, *58*, 6166–6171.
40. Dejneka, M.; Snitzer, E.; Riman, R.E. Blue, green and red fluorescence and energy transfer of Eu^{3+} in fluoride glasses. *J. Lumin.* **1995**, *65*, 227–245.
41. Yordanova, A.; Milanova, M.; Iordanova, R.; Fabian, M.; Aleksandrov, L.; Petrova, P. Network Structure and Luminescent Properties of ZnO–B_2O_3–Bi_2O_3–WO_3: Eu^{3+} Glasses. *Materials* **2023**, *16(20)*, 6779.

 doi:10.20944/preprints202601.0022.v1

42. Milanova, M.; Aleksandrov, L.; Yordanova, A.; Iordanova, R.; Tagiara, N.S.; Herrmann, A.; Gao, G.; Wondraczek, L.; Kamitsos, E.I. Structural and luminescence behavior of Eu^{3+} ions in ZnO-B_2O_3-WO_3 glasses. *J. Non-Cryst. Solids* **2023**, *600*, 122006.
43. Iordanova, R.; Milanova, M.; Yordanova, A.; Aleksandrov, L.; Nedyalkov, N.; Kukeva, R.; Petrova, P. Structure and Luminescent Properties of Niobium-Modified ZnO-B_2O_3:Eu^{3+} Glass. *Materials* **2024**, *17*, 1415.
44. Oomen E.W.J.L.; Dongen A.M.A. Europium (III) in oxide glasses: dependence of the emission spectrum upon glass composition. *J. Non-Cryst. Solids* **1989**, *111*, 205-213.
45. Bettinelli, M.; Speghini, A.; Ferrari, M.; Montagna, M. Spectroscopic investigation of zinc borate glasses doped with trivalent europium ions. *J. Non-Cryst. Solids* **1996**, *201*, 211–221.
46. Annapurna, K.; Das, M.; Kundu, M.; Dwivedhi, R.N.; Buddhudu, S. Spectral properties of Eu^{3+}: ZnO–B_2O_3–SiO_2 glasses. *J. Mol. Struct*. **2005**, *741*, 53–60.
47. Reddy, B. N. K., Raju, B. D., Thyagarajan, K., Ramanaiah, R., Jho, Y. D., Reddy, B. S. Optical characterization of Eu^{3+} ion doped alkali oxide modified borosilicate glasses for red laser and display device applications. *Ceram. Int.* **2017**, *43(12)*, 8886-8892.
48. Azeem, P. A., Kalidasan, M., Gopal, K. R., Reddy, R. R. Spectral analysis of Eu^{3+}: B_2O_3–Al_2O_3–MF2 (M= Zn, Ca, Pb) glasses. *J. Alloys Compd.* **2009**, *474(1-2)*, 536-540.
49. Bajaj, R., Rao, A. S., & Prakash, G. V. Photoluminescence down-shifting studies of thermally stable Eu^{3+} ions doped borosilicate glasses for visible red photonic device applications. *J. Non-Cryst. Solids* **2022**, *575*, 121184.
50. Nandyala, S. H., Hungerford, G., Santos, J. D., Walsh, B. M., Di Silvio, L., Stamboulis, A. Time-resolved and excitation-emission matrix luminescence behaviour of boro-silicate glasses doped with Eu^{3+} ions for red luminescent application. *Mater. Res. Bull.* **2021**, *140*, 111340.
51. Song, H.; Chen, B.; Sun, B.; Zhang, J.; Lu, S. Ultraviolet light-induced spectral change in cubic nanocrystalline Y_2O_3: Eu^{3+}. *Chem. Phys. Lett.* **2003**, *372(3-4)*, 368-372.
52. Kabir, M.; Ghahari, M.; Afarani, M. S. Co-precipitation synthesis of nano Y_2O_3: Eu^{3+} with different morphologies and its photoluminescence properties. *Ceram. Int.* **2014**, *40(7)*, 10877-10885.
53. Wu, L.; Zhang, F.; Wu, L.; Yi, H.; Wang, H.; Zhang, Y.; Xu, J. Structure refinement and one-center luminescence of Eu^{3+} activated $ZnBi_2B_2O_7$ under UV excitation. *J. Alloys Compd.* **2015**, *648*, 500–506.
54. Binnemans, K.; Gorller-Walrand, C. Application of the Eu^{3+} ion for site symmetry determination. *J. Rare Earths* **1996**, *14*, 173–180.
55. Smith, T.; Guild, J. The CIE colorimetric standards and their use. *Trans. Opt. Soc.* **1931**, *33*, 73.
56. Paolini, T.B. SpectraChroma (Version 1.0.1) [Computer Software]. 2021. Available online: https://zenodo.org/records/4906590 (accessed on 7 June 2021).
57. Trond, S.S.; Martin, J.S.; Stanavage, J.P.; Smith, A.L. Properties of Some Selected Europium—Activated Red. *J. Electrochem. Soc.* **1969**, *116*, 1047–1050.